

Supporting Information

Changyong Lan^a, Chun Li^{a,*}, Shuai Wang^a, Yi Yin^a, Huayang Guo^a, Nishuang Liu^b
and Yong Liu^a

^a State Key Laboratory of Electronic Thin Film and Integrated Device, School of Optoelectronic Information, University of Electronic Science and Technology of China, Chengdu 610054, China

^b Wuhan National Laboratory for Optoelectronics Huazhong University of Science and Technology, Wuhan 430074, China

1. Characterization

1.1 Characterization methods

The X-ray diffraction (XRD) pattern of ZnO film was collected by X-ray diffractometer (Bruker D8) with a Cu K α radiation. The high resolution transmission electron microscopy (HRTEM) image and selected area electron diffraction (SAED) of monolayer WS₂ were obtained using transmission electron microscopy (JEOL-3000F). Raman spectrometer (Andor, SR-5001-A-R) with a green laser (532 nm) was used to get Raman spectra of the samples. The optical microscopy image of monolayer WS₂ was obtained using a microscope (Shanghai Optical Instrument Factory, 6XD-3).

*Author to whom any correspondence should be addressed. E-mail: lichun@uestc.edu.cn

1.2 Results and Discussion

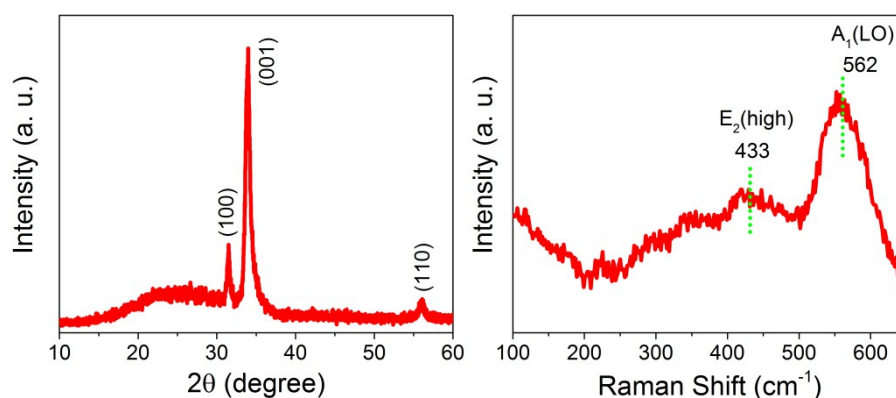


Figure S1. Characterization of ZnO film. (a) XRD pattern. (b) Raman spectrum.

The poor crystallinity of ZnO film can be derived from its XRD pattern and Raman spectrum as shown in figure S1. The diffraction peaks from ZnO film are not very strong as shown in figure S1(a), which leads to the observation of non-crystalline wide peak (centered at about 24°) from glass substrate. We can derive grain size from Scherrer equation $d=0.89\lambda/\beta\cos\theta$ using the XRD pattern, where d is the grain size, λ is the wavelength of the X-ray, β is the line broadening at half the maximum intensity, θ is the Bragg angle. The grain size derived from Scherrer equation is about 12 nm, indicating the poor crystallinity of the ZnO film. We also measured the Raman spectrum (shown in figure S1(b)) of the ZnO film, and the Raman peaks from ZnO are broad, which also confirms the poor crystallinity of the ZnO film.

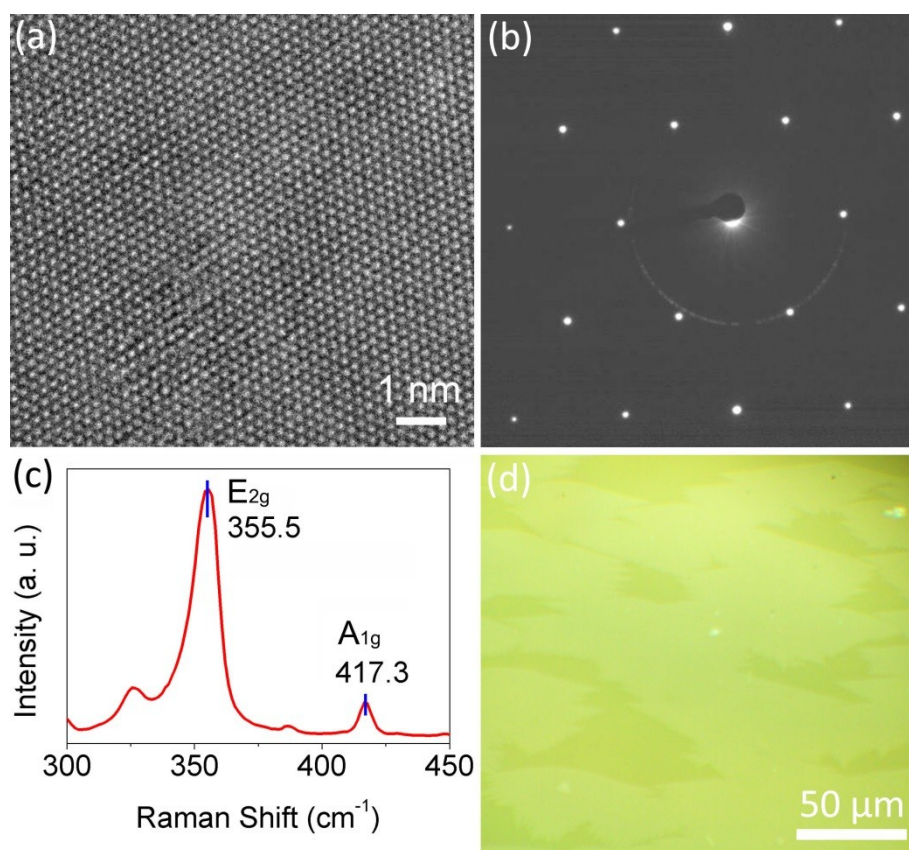


Figure S2 Characterization of monolayer WS₂. (a) HRTEM image. (b) SAED pattern. (c) Raman spectrum. (d) Optical microscopy image.

The crystallinity of monolayer WS₂ can be derived from HRTEM image and SAED as shown in figure S2(a) and S2(b). The clear lattice fringes and clear diffraction spots indicate the high crystallinity of the monolayer. And the sharp Raman peaks from the monolayer WS₂ shown in figure S2(c) also confirms the high crystallinity of the monolayer WS₂. The size of the monolayer WS₂ can be roughly estimated from the non-continuous sample (shown in figure S2(d)), which suggests the single domain size of monolayer WS₂ is about 30-50 μm. The results indicate the high quality of the monolayer WS₂.

2. Comparison of photoresponse of monolayer WS₂ with ZnO and ZnO-WS₂ heterostructure devices

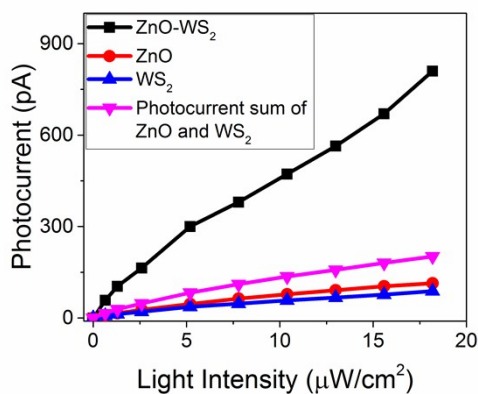


Figure S3. Photocurrent as a function of light intensity with the wavelength of 340 nm in air.

As can be seen in figure S3, the photocurrent of monolayer WS₂ is a little smaller than that of ZnO. The photocurrent sum of monolayer WS₂ and ZnO is much smaller than that of the ZnO-WS₂ heterostructure. So the charge transfer between the ZnO and the monolayer WS₂ should be considered. For example, the photocurrent of ZnO-WS₂ heterostructure is about 815 pA when the light intensity is 18.2 $\mu\text{W}/\text{cm}^2$, while the sum of photocurrent from ZnO and monolayer WS₂ is only 200 pA under the same light intensity.

3. Deposition of ZnMgO film and fabrication of photoconductive devices

ZnMgO was deposited by reactive radio frequency magnetron sputtering technique using Zn target and Mg disks as Zn source and Mg source, respectively. Quartz glass was used as substrate. Before sputtering, the pressure of the chamber was pumped to 4×10^{-4} Pa. The substrate temperature and chamber pressure during the

sputtering process were 500 °C and 0.36 Pa, respectively. The gas flow rate ratio of O₂ : Ar was 3:2. The sputtering power was 100 W and the sputtering time was 1.5 h. The fabrication of ZnMgO and ZnMgO-WS₂ heterostructure photoconductive devices is similar with that of ZnO and ZnO-WS₂ heterostructure devices.

4. Photoresponse of ZnMgO and ZnMgO heterostructure devices

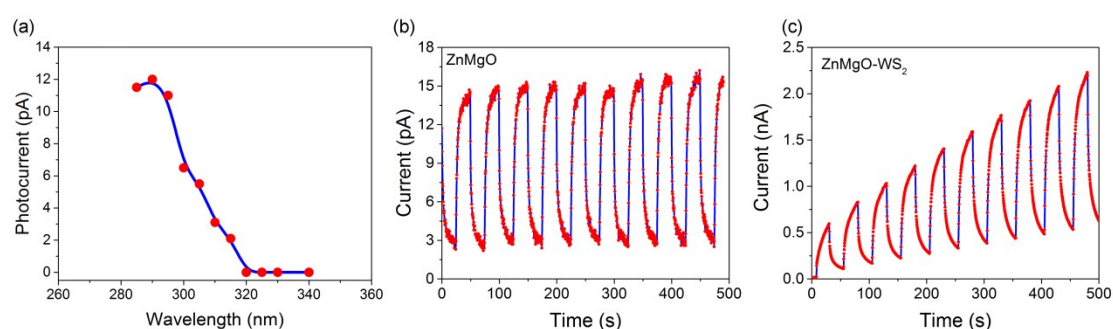


Figure S4. (a) Photocurrent as a function of wavelength. The light intensity for each measured point is 3.98 $\mu\text{W}/\text{cm}^2$. (b) and (c) Current vs. time with chopped light. The light wavelength is 290 nm and the intensity is 3.98 $\mu\text{W}/\text{cm}^2$. (b) ZnMgO, (c)

ZnMgO-WS₂ heterostructure.

The photocurrent as a function of wavelength is shown in figure S4(a), which indicates the band-gap related cut off wavelength of about 320 nm, suggesting the band-gap of ZnMgO is about 3.88 eV. So the band gap of ZnMgO is larger than that of ZnO (3.2 eV), indicating that Mg is indeed doped into ZnO. The current of ZnMgO as a function of time with chopped light is shown in figure S4(b). The photocurrent is about 12 pA when the light intensity is 3.98 $\mu\text{W}/\text{cm}^2$, which is very small. The photocurrent of ZnMgO is very stable as can be seen from figure S4(b). In contrast,

for ZnMgO-WS₂ heterostructures as shown in figure S4(c), the photocurrent is on the order of nA, which is much larger than that of ZnMgO. The increase of photocurrent upon light illumination is ascribed to persistent photoconductive effect, which is a common phenomenon observed in ZnO related films. The persistent photoconductive effect may be caused by defects in ZnMgO, which needs further investigation.